Acta Oceanol. Sin., 2022, Vol. 41, No. 4, P. 146–156
https://doi.org/10.1007/s13131-021-1827-x
http://www.aosocean.com
E-mail: ocean2@hyxb.org.cn

Spatio-temporal analysis of the melt onset dates over Arctic sea ice from 1979 to 2017

Shuang Liang[1, 3], Jiangyuan Zeng[2*], Zhen Li[1], Dejing Qiao[4]

[1] Key Laboratory of Digital Earth Science, Aerospace Information Research Institute, Chinese Academy of Sciences, Beijing 100094, China

[2] State Key Laboratory of Remote Sensing Science, Aerospace Information Research Institute, Chinese Academy of Sciences, Beijing 100101, China

[3] University of Chinese Academy of Sciences, Beijing 100049, China

[4] College of Surveying and Geo-Informatics, North China University of Water Resources and Electric Power, Zhengzhou 450045, China

Received 10 November 2020; accepted 8 February 2021

Abstract

The melt onset dates (MOD) over Arctic sea ice plays an important role in the seasonal cycle of sea ice surface properties, which impacts Arctic surface solar radiation absorbed by the ice-ocean system. Monitoring interannual variations in MOD is valuable for understanding climate change. In this study, we investigated the spatio-temporal variability of MOD over Arctic sea ice and 14 Arctic sub-regions in the period of 1979 to 2017 from passive microwave satellite data. A set of mathematical and statistical methods, including the Sen's slope and Mann-Kendall mutation tests, were used to comprehensively assess the variation trend and abrupt points of MOD during the past 39 years for different Arctic sub-regions. Additionally, the correlation between Arctic Oscillation (AO) and MOD was analyzed. The results indicate that: (1) all Arctic sub-regions show a trend toward earlier MOD except the Bering Sea and St. Lawrence Gulf. The East Siberian Sea exhibits a significantly earlier trend, with the highest rate of –9.45 d/decade; (2) the temporal variability and statistical significance of MOD trend exhibit large interannual differences with different time windows for most regions in the Arctic; (3) during the past 39 years, the MOD changed abruptly in different years for different sub-regions; (4) the seasonal AO has more influence on MOD than monthly AO. The findings in this study can improve our knowledge of MOD changes and are beneficial for further Arctic climate change study.

Key words: Arctic sea ice, melt onset dates, spatio-temporal analysis, abrupt changes, Arctic Oscillation

Citation: Liang Shuang, Zeng Jiangyuan, Li Zhen, Qiao Dejing. 2022. Spatio-temporal analysis of the melt onset dates over Arctic sea ice from 1979 to 2017. Acta Oceanologica Sinica, 41(4): 146–156, doi: 10.1007/s13131-021-1827-x

1 Introduction

The global temperature has continued to rise since the 1970s, which has a profound impact on the Arctic region, leading to a gradual warming of the Arctic (Cohen et al., 2014; Pachauri et al., 2014). Sea ice, as an integral component of the Arctic climate system (Aagaard and Carmack, 1989; Barry et al., 1993; Box et al., 2019; Wang et al., 2019), has undergone rapid changes in recent decades (Bi et al., 2016; Lemke et al., 2007; Stroeve and Notz, 2018). The melt onset dates (MOD) over Arctic sea ice can be used to depict the capability of the absorption of solar energy by the sea ice surface (Perovich et al., 2007), which significantly influences the Arctic surface radiation energy balance between sea ice and atmosphere (Belchansky et al., 2004a; Bliss et al., 2019; Perovich et al., 2007). During the melt season, the sea ice surface meltwater triggers a decrease in surface albedo, resulting in more solar energy absorbed by the sea ice surface and accelerating the reduction of sea ice volume (Curry et al., 1995; Stroeve et al., 2014). Consequently, an improved understanding of the spatio-temporal characteristics of the MOD variations at multiple time scales would contribute to assess the responses of Arctic sea ice to climate change in the future and predict the trend of Arctic sea ice MOD.

Due to the limited *in situ* observations, passive microwave remote sensing has become one of the most viable methods for monitoring MOD, which provides observation with all-time and all-weather coverage, especially in polar areas with the complex geographical environment and extreme climatic conditions (Markus et al., 2009; Smith, 1998). When liquid water appears in sea ice, the microwave emission measured by microwave sensors will change rapidly, and thus detects the earliest initiation of melt (Anderson, 1987). Although data from active microwave sensors can yield MOD with a reasonably high spatial resolution (100 m–5 km) (Kwok et al., 2003; Winebrenner et al., 1994), it is more common to estimate MOD from passive microwave brightness temperature (Belchansky et al., 2004b; Drobot and Anderson, 2001a; Smith, 1998), which can provide a consistent long-term observation record over the entire Arctic from 1979 onwards. Several MOD estimation algorithms have been developed based

Foundation item: The National Key Research and Development Program of China under contract No. 2018YFA0605403; the National Natural Science Foundation of China under contract No. 42071084; Jiangyuan Zeng was supported by the Youth Innovation Promotion Association CAS under contract No. 2018082.

*Corresponding author, E-mail: zengjy@radi.ac.cn

on passive microwave observations, including the advanced horizontal range algorithm (AHRA) (Drobot and Anderson, 2001b), the passive microwave method (Markus et al., 2009), and the combination of active and passive microwave data (Belchansky et al., 2004a), which have been successfully applied in the study of MOD over Arctic sea ice (Bliss et al., 2017). Some studies have reported different discoveries of MOD by using passive microwave products. Mortin et al. (2016) found the sea ice in the Arctic is experiencing an earlier melt onset over the past few decades. Moreover, the magnitude and trend of MOD vary with location and periods. Anderson and Drobot (2001) reported the MOD in the western central Arctic exhibited a significant earlier trend (8.9 d/decade, p<0.05), and the Beaufort Sea and Canadian Archipelago regions significantly advanced by 5.1 d/decade and 6.7 d/decade during 1979–1998, respectively. Stroeve et al. (2006) indicated the MOD displayed a significant earlier trend at a rate of 4.7 d/decade in the Beaufort Sea, 7.3 d/decade in the Kara, and 8.8 d/decade in the Barents from 1979 to 2005. Bliss and Anderson (2014a) identified the interannual mean of MOD from 1979 to 1987 was generally later than that during 1979–2012. Several studies pointed out that the interannual variations of MOD are likely related to many factors, such as atmospheric circulation (Drobot and Anderson, 2001b), surface downwelling longwave radiation (Barber and Thomas, 1998; Maksimovich and Vihma, 2012), and atmospheric moisture anomalies (Mortin et al., 2016). The abovementioned studies only focused on the interannual variations of MOD, while few studies have reported the results concerning the mutation monitoring of MOD variations over the Arctic so far. Additionally, some studies have preliminarily indicated the Arctic Oscillation (AO) has effects on MOD variation (Belchansky et al., 2004b; Drobot and Anderson, 2001a); however the correlation analysis between AO and MOD for different Arctic sub-regions is limited and is worthy of further investigation.

Therefore, in this study, more comprehensive statistical analysis, such as mutation detection and trend analysis of MOD variations, was conducted. The spatio-temporal variation characteristics of MOD for Arctic sea ice over a 39 years period (1979–2017) during the melt seasons were analyzed by using long-term passive microwave observations. The time-series approach (Sen's slope estimator) was used to analyze the spatio-temporal variable patterns and trends for the Arctic and its 14 sub-regions from 1979 to 2017. A multi-time scales analysis of the trend variations of MOD was performed. Additionally, the Mann-Kendall (M-K) mutation test was adopted to investigate the transition point for different Arctic sub-regions. Finally, the correlation between monthly and seasonal AO and MOD was investigated. The paper is organized as follows. The MOD dataset and study region are briefly introduced in Section 2. Section 3 describes the analysis method used in the study, including the Sen's slope estimator, the M-K method, and the correlation analysis. In Section 4, the spatial and temporal variation characteristics, different period variations, and transition point of MOD, and the correlation between MOD and AO for the Arctic and its sub-regions are analyzed. Finally, the conclusions are summarized in Section 5.

2 Data and study area

2.1 *MOD dataset*

The MOD data used in the study are the "Snow Melt Onset Over Arctic Sea Ice from SMMR and SSM/I-SSMIS Brightness Temperatures, Version 4", which are available from the National Snow and Ice Data Center (NSIDC) (https://nsidc.org/data/nsidc-0105) (Anderson et al., 2019). The data are provided in a polar stereographic grid with a spatial resolution of 25 km. In this study, the annual MOD in the period of 1979 to 2017 was used. The operational MOD algorithm for this data is the AHRA developed by Drobot and Anderson (2001b). No other change is made to the AHRA method since the publication by Bliss and Anderson (2014b) and thus, the V3 (Meier et al., 2017) and V4 data have almost no difference at all in most sea ice areas. The MOD in the new version is reprocessed by using a new version of the sea ice extent masks. In the dataset, the brightness temperatures from several passive microwave sensors are collected, including the scanning multichannel microwave radiometer (SMMR) during 1979 to 1987, the special sensor microwave imagers (SSM/I) and the special sensor microwave imager and sounder (SSMIS) during 1988 to 2017 to estimate the MOD over Arctic sea ice. To ensure consistent input data record, prior to determining the MOD over sea ice, the brightness temperature data from different platforms are calibrated using the DMSP F08 SSM/I as the baseline sensor through linear regression coefficients during overlap periods following previous studies (Abdalati et al., 1995; Jezek et al., 1991; Stroeve et al., 1998).

The earliest MOD can be identified by a change in the brightness temperature. Briefly, the theoretical basis of the AHRA method depends on the day-to-day variability in the increase of brightness temperature (Drobot and Anderson, 2001a). Furthermore, horizontal channels are more strongly related to snow conditions during melt than vertical channels. Moreover, different frequencies have different responses to melt onset. The change of brightness temperature at 19 GHz (18 GHz for SMMR data) is more dramatic than that at 37 GHz when the liquid water occurring in the snowpack. Therefore, the melt criterion of the AHRA method to detect MOD is the daily difference between horizontally polarized brightness temperature at 19 GHz (18 GHz for SMMR data) and 37 GHz channels (Drobot and Anderson, 2001a). For more details of the AHRA method, readers are referred to Drobot and Anderson (2001a). The MOD data set released by NSIDC has been used in many previous studies (Bliss and Anderson, 2014b, 2018; Singh et al., 2020). Some studies have confirmed and explained the accuracy of the MOD data (Bliss and Anderson, 2018; Drobot and Anderson, 2001a).

2.2 *Study area*

To better understand the temporal variability of the MOD in different regions, the Arctic region was divided into 14 sub-regions (i.e., Sea of Okhotsk, Bering Sea, Hudson Bay, St. Lawrence Gulf, Baffin Bay, Greenland Sea, Barents Sea, Kara Sea, Laptev Sea, East Siberian Sea, Chukchi Sea, Beaufort Sea, Canadian Archipelago, and central Arctic) following the criterion used in Bliss and Anderson (2018). The Arctic region defined here is relatively broad, spanning the Arctic Circle and the middle and low latitudes, which is identical to the region definitions used by Meier et al. (2017). Figure 1 shows the Arctic and its sub-regions analyzed in the study. The version of the Arctic section mask file used in the study also first appeared in Meier et al. (2017). The original section mask file is an array formatted to NSIDC's 25 km Northern Hemisphere Polar Stereographic Grid, and we classified MOD into 14 sub-regions according to the mask file.

3 Methods

3.1 *Trend test method*

In this study, the Sen's slope estimator (Sen, 1968) and the M-K trend test (Kendall, 1948) were used to investigate the temporal trends of MOD and its significance over the Arctic from 1979 to

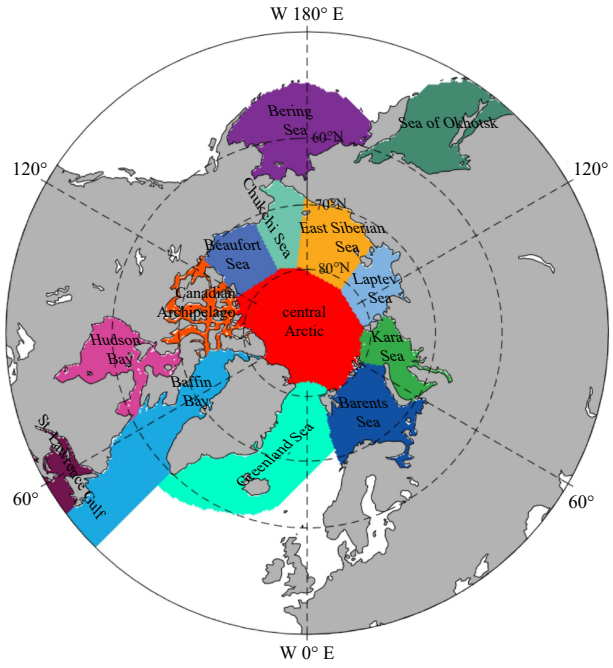

Fig. 1. Arctic and its sub-regions analyzed in the study. Different colors indicate different Arctic sub-regions and land is in gray.

2017 at the pixel level. The Sen's slope estimator can not only reduce the interference of abnormal values in a time series but also diminish the influence of missing time series observations and non-normally distributed data (Liuzzo et al., 2016). Therefore, Sen's slope estimator is widely used to analyze long-term sequence datasets. It is often used in the trend analysis of long-term series data to detect the magnitude of the trend:

$$\text{sen} = \text{Median}\left(\frac{x_j - x_k}{j-k}\right), \quad j = 1, 2, \cdots, n, \tag{1}$$

where x_j and x_k are the data values at times j and k (j>k), respectively. A positive sen value indicates an increasing trend, and a negative sen value indicates a decreasing trend.

The M-K trend test is a nonparametric test method, which has no requirement on data type and is often applied to determine the significance. The standard normal statistic of the M-K test (Z) can be calculated by

$$Z = \begin{cases} \dfrac{s-1}{\sqrt{\text{Var}(S)}} & \text{if } S > 0 \\ 0 & \text{if } S = 0 \\ \dfrac{s+1}{\sqrt{\text{Var}(S)}} & \text{if } S < 0 \end{cases}, \tag{2}$$

where

$$S = \sum_{i=1}^{n-1} \sum_{j=i+1}^{n} \text{sgn}\left(x_j - x_i\right), \tag{3}$$

$$\text{sgn}\left(x_j - x_i\right) = \begin{cases} +1 & \text{if } x_j - x_i > 0 \\ 0 & \text{if } x_j - x_i = 0 \\ -1 & \text{if } x_j - x_i < 0 \end{cases}, \tag{4}$$

$$\text{Var}(S) = \frac{n(n-1)(2n+5) - \sum_{i=1}^{m} t_i (t_i - 1)(2t_i + 5)}{18}, \tag{5}$$

where x_i and x_j indicate the pixels values at times i and j, respectively; sgn(x_j–x_i) represents the sign function; n and m are the number of data points and tied groups, respectively; t_i denotes the number of ties of extent i.

3.2 *Mutation test method*

The M-K method was also employed to detect the mutation points of MOD over the Arctic region and its sub-regions. The M-K method is considered to be an effective method for detecting the transition point from a relatively stable state to another state (Da Silva et al., 2015; Fu et al., 2013).

For a time series $x_i = (x_1, x_2, \cdots, x_n)$, the statistic S_k can be calculated as follow:

$$S_k = \sum_{i=1}^{k} r_i, \quad k = 2, 3, \cdots, n, \tag{6}$$

where

$$r_i = \begin{cases} 1, & x_i > x_j \\ 0, & x_i \leqslant x_j \end{cases}, \ j = 1, 2, \cdots, i. \tag{7}$$

Assuming that the time series x_i is random and independent, the statistic is defined as

$$\text{UF}_k = \frac{[S_k - E(S_k)]}{\sqrt{\text{Var}(S_k)}}, \quad k = 1, 2, \cdots, n, \tag{8}$$

where

$$E(S_k) = \frac{n(n-1)}{4}, \tag{9}$$

$$\text{Var}(S_k) = \frac{n(n-1)(2n+5)}{72}, \tag{10}$$

where S_k is the cumulative number of cases x_i>x_j ($1 \leqslant j \leqslant i$), n is the number of samples, UF_i follows a standard normal distribution, and UF_1=0. If UF_i value is greater than 0, it denotes an upward trend; otherwise, it denotes a downward trend. If UF_i value exceeds the significance level, it indicates that there is a significant trend in the time series.

Moreover, this method also calculates the statistic UB_k for the inverse series (x_n, x_{n-1}, ···, x_1) following the same procedures as shown in Eqs (6)–(10), and UB_1=0. The intersection of the UF_k and UB_k curves in confidence interval is determined as the mutation point.

3.3 *Correlation analysis*

The AO is a large scale mode of climate variability, also referred to as the Northern Hemisphere annular mode. It is not only an important parameter predicting El Niño (Chen et al., 2014), but also naturally has a great influence on the general Arctic climate (Moritz et al., 2002; Jevrejeva et al., 2003). Previous studies have explored the impact of AO on the MOD over the Arctic sea ice (Belchansky et al., 2004b; Drobot and Anderson,

2001a), sea ice motion (Rigor et al., 2002), and surface air temperature (Rigor et al., 2000). To further investigate the effect of AO on MOD changes in Arctic sub-regions, we calculated Pearson correlation coefficient between monthly and seasonal MOD and AO. The AO index is from NOAA National Centers for Environmental Information, which is obtained by projecting the AO loading pattern to the daily anomaly 1 000 hPa height field over 20°–90°N latitude. Besides, winter, spring, and summer here are defined as January–March, April–June, and July–September, respectively. The monthly mean AO index from 1979 to 2017 was used in this study and the seasonal AO index was calculated from the monthly mean AO index. More information of the AO index data can be seen at http://ncdc.noaa.gov/teleconnections/ao/.

4 Results and discussion

4.1 *Spatial pattern of MOD*

The spatial patterns of MOD from 1979 to 2017 are shown in Fig. 2, which is described by mean values, standard deviation, trend, and significance. The processing method of data is the same as Bliss and Anderson (2014b). All statistics were calculated on a per-pixel basis where the MOD exists in all 39 years of the data record. A pole hole area (>84.5°N) is observed in Fig. 2 since data were not collected by the SMMR sensor within this region, and those pixels have been discarded from the subsequent statistical analysis. During the past 39 years, the mean MOD on Arctic sea ice has noticeable regional differences. The MOD occurs earlier at low latitude (<70°N), and the MOD gradually increases with increasing latitude spatially. In addition, the MOD mostly ranges from 90 to 170 day of year (DOY), accounting for 87.9% of the study area. The earlier MOD is found in the peripheral sea ice (Sea of Okhotsk, Bering Sea, Hudson Bay and St. Lawrence Gulf) and the southernmost regions, with occurrence before 100 DOY (April 9). However, a small area in the Canadian Archipelago and northwestern coast of Greenland shows later MOD around late May. By contrast, the regions with later MOD, occurring in above 150 DOY (May 30), are mainly located in the central Arctic and a part of the Canadian Archipelago.

Overall, most regions (81.7% of the study area) have considerable inter-annual variability as reflected by the high standard deviation (more than 15 days). Specifically, the regions with the largest standard deviation (more than 40 days) are located in the ice edge of the Laptev Sea and Kara Sea, indicating that the MOD in these regions fluctuates more significantly during the past 39 years. However, a part of study area (about 2.3%), mainly distributed in the western parts of the central Arctic, the Canadian Archipelago, the edge of Sea of Okhotsk and parts of Laptev Sea, exhibits a smaller variability within 10 days. The spatial pattern of MOD is consistent with that in Bliss and Anderson (2014b), though there is a slight difference in study period.

The spatial pattern of the change trends of MOD is displayed in Fig. 2c. Over the past 39 years (from 1979 to 2017), there are noticeably larger areas experiencing advanced MOD than those with delayed trends. Specifically, 85.9% of the study area shows an earlier trend (58.2% are statistically significant), while 14.1% of those exhibits a delaying trend (1.2% are statistically significant). Concurrently, 60% of study areas with advanced MOD (>8 d/decade) at the statistically significant level of p<0.05 mainly occur in higher latitude (above 70°N) and the northern part of Hudson Bay, whereas more than 1.2% of delayed MOD (>8 d/decade) at the significance level of p<0.05 occur in the northeast of Hudson Bay and eastern coast of Greenland Sea.

4.2 *Variations of MOD in different Arctic sub-regions*

The temporal variations in the MOD were analyzed with Sen's slope estimator based on the mean annual MOD trends, and the trend significance was determined by using the p-value from the two-tailed student's t-test after testing for normal distribution and auto-correlation. Additionally, the coefficient of determination (R^2) between MOD and year was estimated for each region.

Figure 3 presents the mean annual MOD for each Arctic subregion. The average MOD statistics for the 14 Arctic sub-regions in the period of 1979 to 2017 are summarized in each subgraph. Over the past 39 years, the MOD exhibits an earlier trend in most Arctic sub-regions. The largest trend is in the East Siberian Sea, with a significant earlier trend of 9.45 d/decade. Anderson and Drobot (2001) also found the East Siberian Sea displayed the earlier MOD from 1979 to 1998 and indicated that it may be caused by different climate regimes due to land or ice-locked area. The regions with earlier trends exceed 7 d/decade, are mainly located in the Barents Sea, Kara Sea, Laptev Sea, Chukchi Sea, and Beaufort Sea, which may due to the large-scale weather patterns (such as a cyclonic activity) (Anderson and Drobot, 2001). In addition, the MOD has a significant trend of –6.97 d/decade in the central Arctic located in the highest latitudes, with a relatively high R^2 value of 0.7. These MOD trends are generally consistent with the findings of Bliss et al. (2019). For the peripheral sea ice regions including the Sea of Okhotsk (Fig. 3a), Hudson Bay (Fig. 3c) and Baffin Bay (Fig. 3e), St. Lawrence Gulf (Fig. 3d), Bering Sea (Fig. 3b) and Greenland Sea (Fig. 3f), the trends are generally smaller, and the R^2 values are relatively low compared to central Arctic (Fig. 3n). Statistically significant trends mainly occur in the Baffin Bay (Fig. 3e) at the significant level of p<0.05 with a low R^2 value of 0.14. In addition, it is interesting to find that the MOD presents delayed trends in the Bering Sea (Fig. 3b) and St. Lawrence Gulf (Fig. 3d) regions typically being statistically different from other regions in the Arctic, with the weaker positive trend of 1.62 d/decade and 0.46 d/decade (in red mark in panels of Fig. 3), respectively. The anomalous results of the Bering Sea are similar to the previous study (Bliss and Anderson, 2014b) and the reasons need to be further investigated.

Compared with the results of Bliss and Anderson , it is found the variation trends of MOD are generally in agreement for the majority of Arctic regions, though the magnitude of change is slightly different. This may be due to the difference in the study period, i.e., 39 years in this study and 34 years in Bliss and Anderson (2014b). The different regional variability is most likely due to the variations of geographical environment and atmospheric conditions for different regions of the Arctic during melting (Bliss and Anderson, 2014a). Figure 4 displays the Pearson correlations between MOD for different Arctic sub-regions, which implies that peripheral seas are nearly independent of each other, whereas the regions in the middle and high latitudes (Barents Sea, Kara Sea, Laptev Sea, East Siberian Sea, Chukchi Sea, Beaufort Sea, Canadian Archipelago, and central Arctic) dominate the variation of MOD in the Arctic.

4.3 *Trend variations of MOD during different periods*

From the above analysis results, the MOD variations not only show pronounced spatial distribution differences but also present distinct temporal heterogeneity. Decadal trends may conceal the strong short-term fluctuations in the MOD. In this section, we analyzed MOD trends with various window sizes (i.e., the length of the study period) ranging from 5 years to 35 years (from 1979 to 2013), across all start-year and window-size combinations, averaged over the Arctic sea ice and its sub-regions,

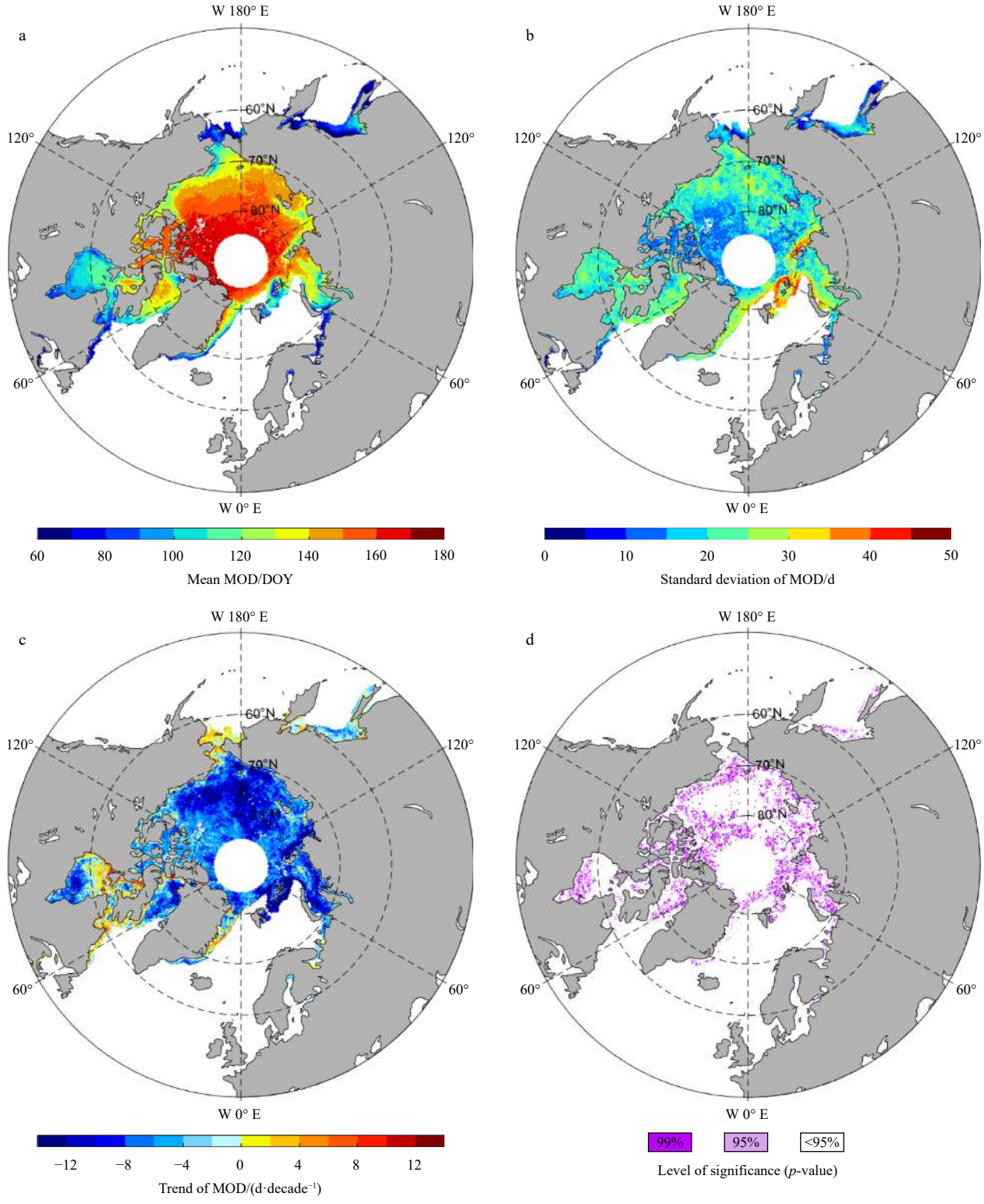

Fig. 2. Spatial distribution of the mean (a) and standard deviation (b) of melt onset dates (MOD) over Arctic sea ice during 1979–2017; c and d represent the trend of MOD and its *p*-values, respectively.

shown in Fig. 5.

The mean annual MOD universally displays earlier trends (i.e., earlier sea ice melt date) for the whole Arctic sea ice, whereas some short-term (5–10 years) changes in MOD demonstrate later trends since the mid-1990s. Meanwhile, the whole Arctic sea ice exhibits larger short-term earlier trends during two periods (1982–1987 and 1999–2001) from Fig. 5o. For Arctic sea ice regions, the change trends of MOD show complex variation characteristics in different study periods, and the trend variations of MOD display noticeable differences in different regions. The trend variations of MOD in peripheral sea ice regions, e.g., Sea of Okhotsk (Fig. 5a), Bering Sea (Fig. 5b), and St. Lawrence Gulf

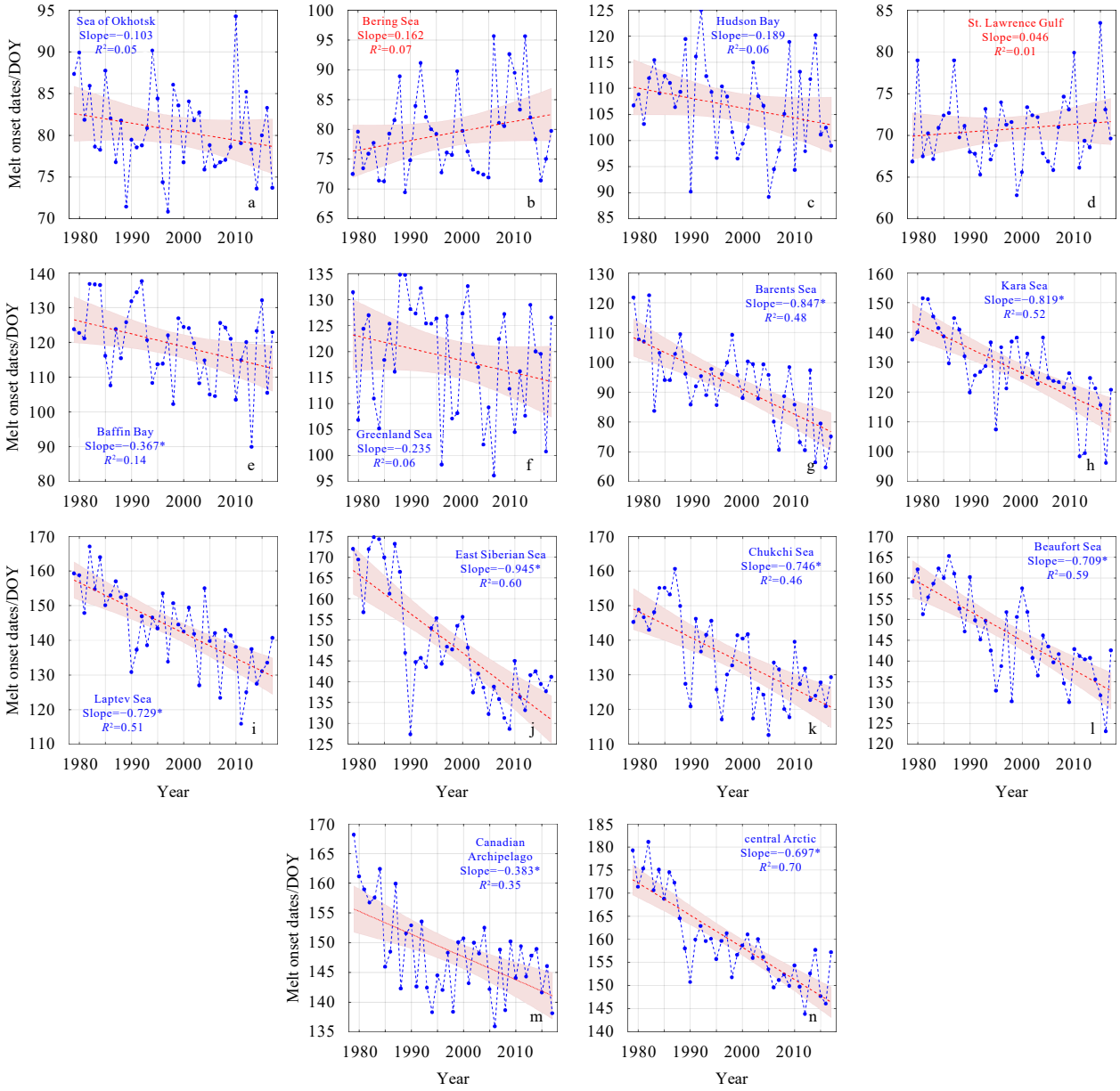

Fig. 3. The trends of the mean annual melt onset dates (MOD) for each Arctic sub-region during the past 39 years (1979–2017). The dots connected by the blue dotted line represent the annual MOD values. The dashed red lines represent the trend lines of the MOD changes. The shaded areas represent the 95% confidence interval of the estimated slope. * indicates statistically significant trends at a 95% confidence level.

(Fig. 5d), are insignificant for different study periods, while the trend of MOD for other sub-regions are significantly positive at time frames of 15–39 years when the study period is before 1985. In addition, we can find the short-term (9–15 years) trend of MOD is significantly negative with a larger change rate (>2 d/a) for Kara Sea (1980–1985) (Fig. 5h), Laptev Sea (1982–1985) (Fig. 5i), East Siberian Sea (1979–1985 and 1997–2000) (Fig. 5j), Chukchi Sea (1983–1986) (Fig. 5k), and Beaufort Sea (1983–1986) (Fig. 5l).

From the multi-time scale analysis of MOD trend, it indicates that the fluctuation of the MOD trend varies with time periods. This also explains the slight difference in the MOD trends in Section 4.2 with those of (Bliss and Anderson, 2014b). As can be seen in Fig. 5, temporal variability and statistical significance of MOD trend exhibit large interannual differences with different time windows for most regions in the Arctic. Thus, when analyzing the long-term changes of MOD, different time scales may get distinctly different results.

4.4 *Mutation analysis of the MOD*

The M-K mutation analysis method was adopted to investigate the abrupt change of MOD. Figure 6 presents the curves of the UF and UB obtained from the M-K mutation test method for the Arctic and its sub-regions from 1979 to 2017, and the 0.05 confidence level was used. If the intersection of the UF and UB curves is between the confidence interval, the time of the intersection corresponds to the time of mutation. It should be noted that the mutation points detected by the M-K method do not mean the minimum or maximum value of a time series data. They represent the trends of the time series data before and after the muta-

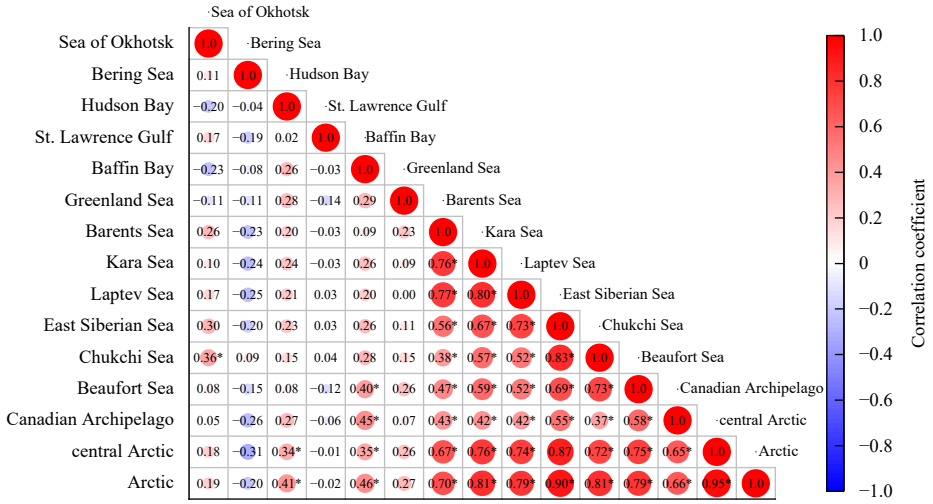

Fig. 4. Pearson correlations between melt onset dates for different Arctic sub-regions. * indicates statistically significant correlation at a 95% confidence level.

tion point are significantly different (Mann, 1945; Kendall, 1948).

First, we analyzed the regional changes in MOD for Arctic sub-regions, see Figs 6a–n. For the Arctic sub-regions, the regions with more than one intersection between UF and UB curves are mainly located in the Bering Sea, Baffin Bay and St. Lawrence Gulf, implying these regions are more prone to abnormal change. Drobot and Anderson (2001a) also found that abnormally late (early) snowmelt onset occurs near the Baffin Bay using principal component analysis. As shown in Fig. 6a, the MOD in the Sea of Okhotsk exhibits a short period of increasing trend (during 1979–1980) and a relatively long period of decreasing trend (after 1981). An abrupt change of MOD in the Sea of Okhotsk is detected in 1982 (significant at the 0.05 level). The MOD in the UF and UB statistic curves has an intersection in 1982 within the confidence interval. The MOD over the Sea of Okhotsk can be separated into two periods. The UF curve of MOD shows an increase before 1982, and then a decrease with fluctuations during 1982–2017, while these trends do not exceed the 95% confidence level. For other peripheral sea ice regions, there are a few intersections of UF and UB curves within the two confidence lines, which indicates that extreme MOD occurs more frequently. The abrupt changes in the Bering Sea occur in 1983, 1986 and 2015 (Fig. 6b). The mutations of the Hudson Bay occur in 1997 and 2013 (Fig. 6c), and those of the Baffin Bay take place in 1988 and 1993, see Fig. 6e. Based on the M-K mutation analysis and change trend analysis, it can be drawn that there is no significant mean annual MOD variation in the St. Lawrence Gulf and Greenland Sea, see Figs 6d and f, respectively. The more mutation points that occur in the St. Lawrence Gulf may be related to the air temperature. The air temperatures are generally warmer in these southerly locations than in other regions (Bliss and Anderson, 2014a). The onset of melting is a sensitive indicator of the near-surface atmospheric conditions, particularly the air temperature.

In contrast to the peripheral sea ice regions, there is only one intersection of UF and UB in 2005 for the Barents Sea (Fig. 6g), 1994 for Chukchi Sea (Fig. 6k), 1993 for Beaufort Sea (Fig. 6l), and 1984 for Canadian Archipelago (Fig. 6m). Additionally, there is a crossing point between the UF and UB curves in 2002 for Kara Sea (Fig. 6h), and 1992 for central Arctic (Fig. 6n). However, both Kara Sea and central Arctic do not have abrupt changes during the study period, because these crossing points do not pass the reliability test of significant level α=0.05.

Overall, as seen in the UF curve, the value of UF statistic is less than 0 for all the study periods except in 1984 (see Fig. 6o), indicating the MOD increases slightly from 1983 to 1984. From the mid 1980s, the MOD displays an earlier trend, and a significant earlier tendency starts at the end of the 1980s. The results of M-K tests show the value of UF exceeds the critical value of −1.96 since 1989, implying that the MOD experiences a significant earlier trend. Further analysis reveals that there is an intersection of UF and UB curves in 1993 in the whole Arctic. However, since the crossing point does not pass the reliability test of significant level α=0.05, it indicates that there are no abrupt changes for MOD over the Arctic sea ice.

As discussed above, the MOD at different Arctic sub-regions displays different mutation points. An extreme MOD variation year in a region may not appear to be an abnormal year of other regions. For example, the mutations of the Sea of the Okhotsk, Bering Sea, Hudson Bay, Baffin Bay, Barents Sea, Chukchi Sea, and Canadian Archipelago do not affect the mutation of the whole Arctic. Therefore, the regional mutation analysis of MOD may be indicative of the close association between MOD variation and the local atmospheric activity (such as cyclone) during the Arctic spring, rather than interaction between regions (Bi et al., 2019; Markus et al., 2009). Bliss and Anderson (2014a) analyzed the effect of cyclonic activity on the MOD and indicated that these small-scale events need to be further investigated to determine how it contributes to ongoing changes in sea ice. Besides, for the entire Arctic, there are no mutation points of MOD occur in the years of obvious sea ice extent minimum such as 2007 and 2012, and thus, the MOD may have no direct contribution toward the retreat of sea ice, which is also mentioned in Markus et al. (2009).

4.5 *Correlation analysis between MOD and AO*

The Pearson correlations between the MOD of Arctic sub-regions and monthly AO can be seen in Fig. 7, which reveals the influence of monthly AO on the MOD of Arctic sub-regions is not significant and shows a weak correlation. The weak correlations between monthly AO and MOD suggest that the MOD over Arctic sea ice is not affected by the short-term effects of AO. Table 1

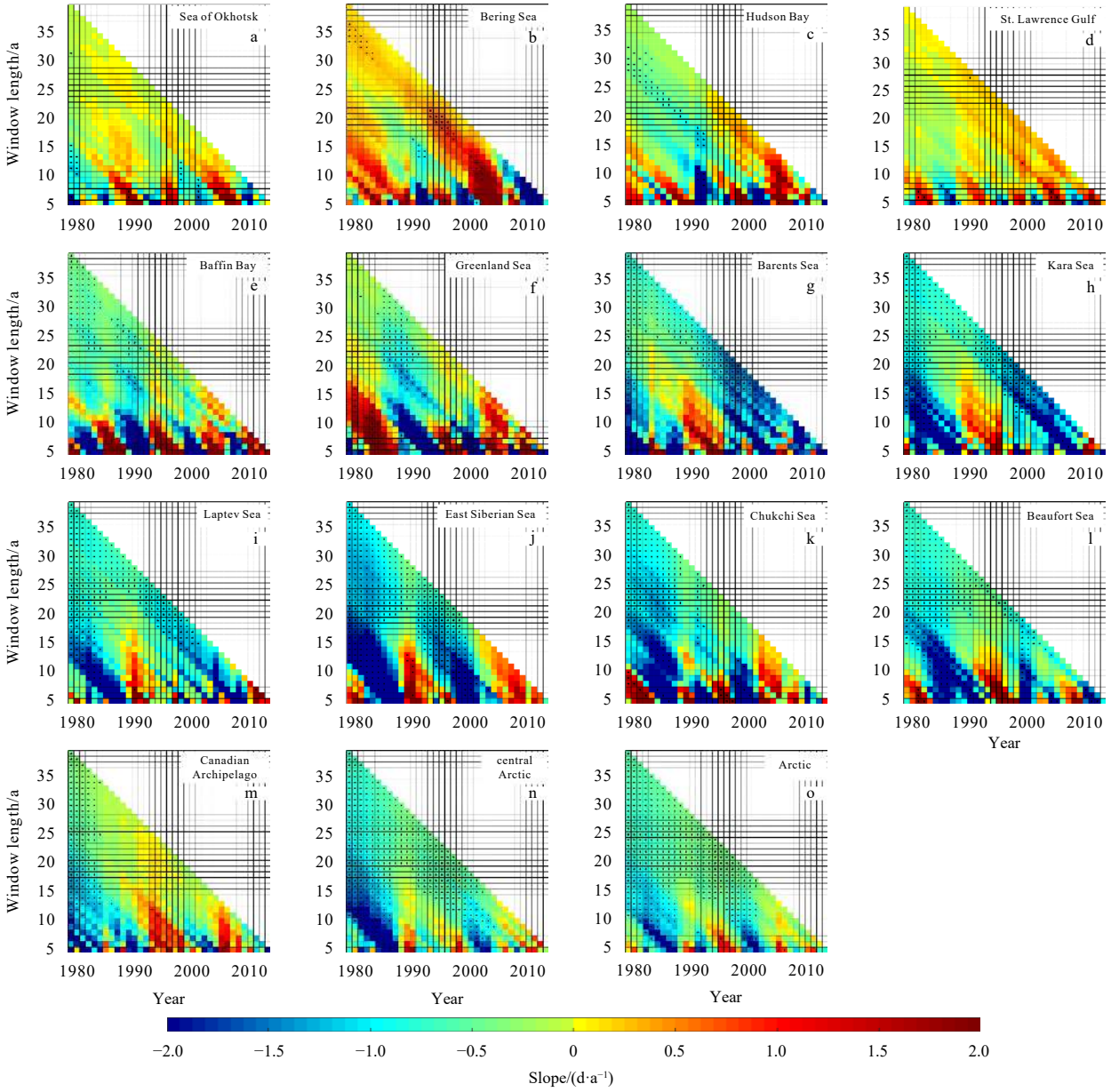

Fig. 5. The variation trends of melt onset dates for different Arctic regions with different window lengths ranging from 5 years to 39 years. The color of pixels indicates the trend of each Arctic sub-region over a single-window size (5 years to 39 years) for each start year (1979–2017). The red (green) color indicates positive (negative) trends. The asterisks * indicate the pixels with statistically significant at 95% confidence level.

illustrates the correlations of seasonal AO and MOD, which indicates that the winter AO has a more significant impact on MOD in portions of Arctic sub-regions. However, snowmelt usually occurs from March to June in the Arctic, implying the lag effect of AO. Baffin Bay and Greenland Sea show positive correlations, whereas other regions (e.g., Sea of Okhotsk, Laptev Sea, East Siberian Sea, and Chukchi Sea) exhibit negative correlations indicating the stronger AO and the earlier MOD. Besides, Drobot and Anderson (2001a) found Baffin Bay and East Siberian Sea have the opposite relationship with AO, which is in good agreement with our results. Some studies pointed out positive (negative) phases of the AO are associated with abnormally warm (cool) surface air temperatures along the Siberian coast (Thompson and Wallace, 1998), which may be the reasons for the positive correlation between AO and MOD. The warmer air temperature contributes to the earlier snowmelt. However, Thompson and Wallace (1998) also indicated abnormally cool (warm) surface air temperatures near Baffin Bay. This may be the reason why Baffin and Greenland exhibit positive correlations, and the cooler air temperature lead to the later MOD over the Arctic sea ice. The weak correlation indicates MOD is not only affected by AO, but may be also associated with other factors, such as air temperature, ocean heat flux, wind fields and clouds.

5 Conclusions

A good knowledge of the spatio-temporal variation of MOD over Arctic sea ice is of keen interest and significance for Arctic climate research. This study systematically investigated the spatio-temporal variation characteristics of annual MOD over the Arctic sea ice from 1979 to 2017, by using a set of mathematical

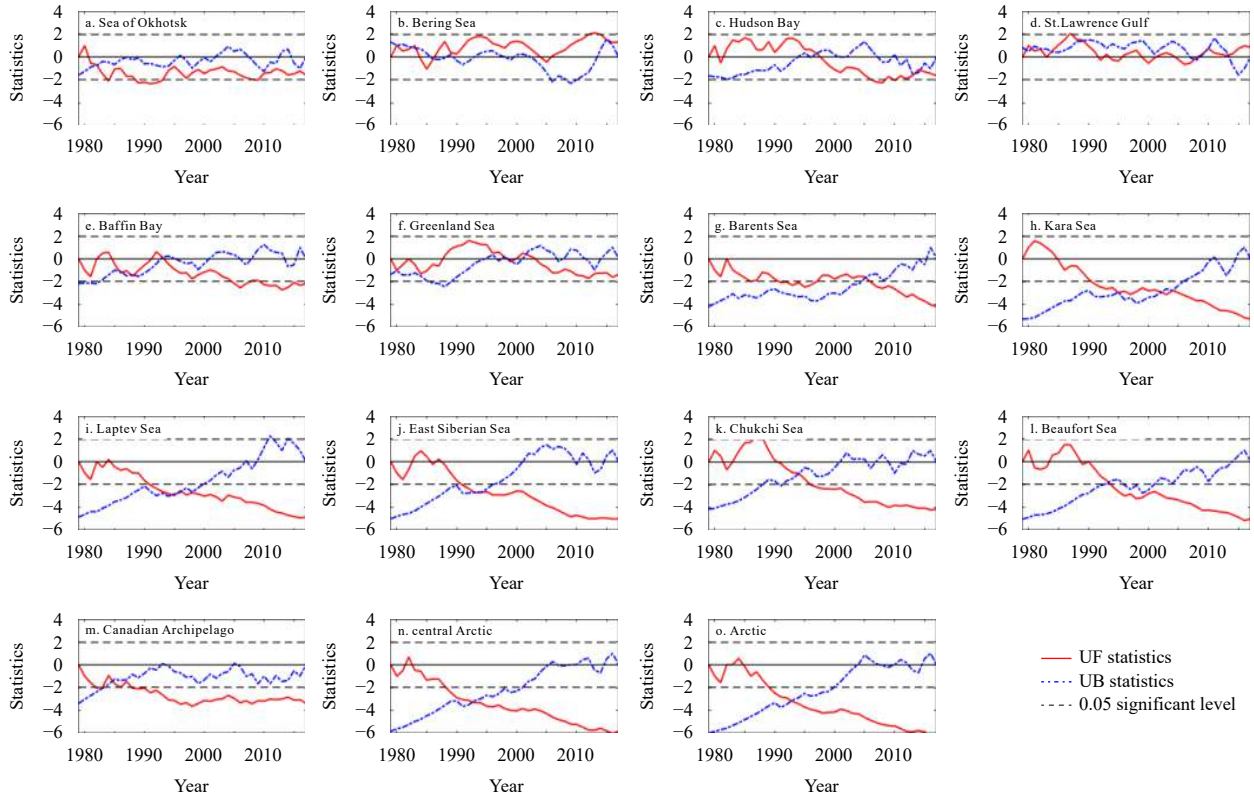

Fig. 6. M-K test of the mean annual melt onset dates for the Arctic and its sub-regions during the past 39 years (1979–2017).

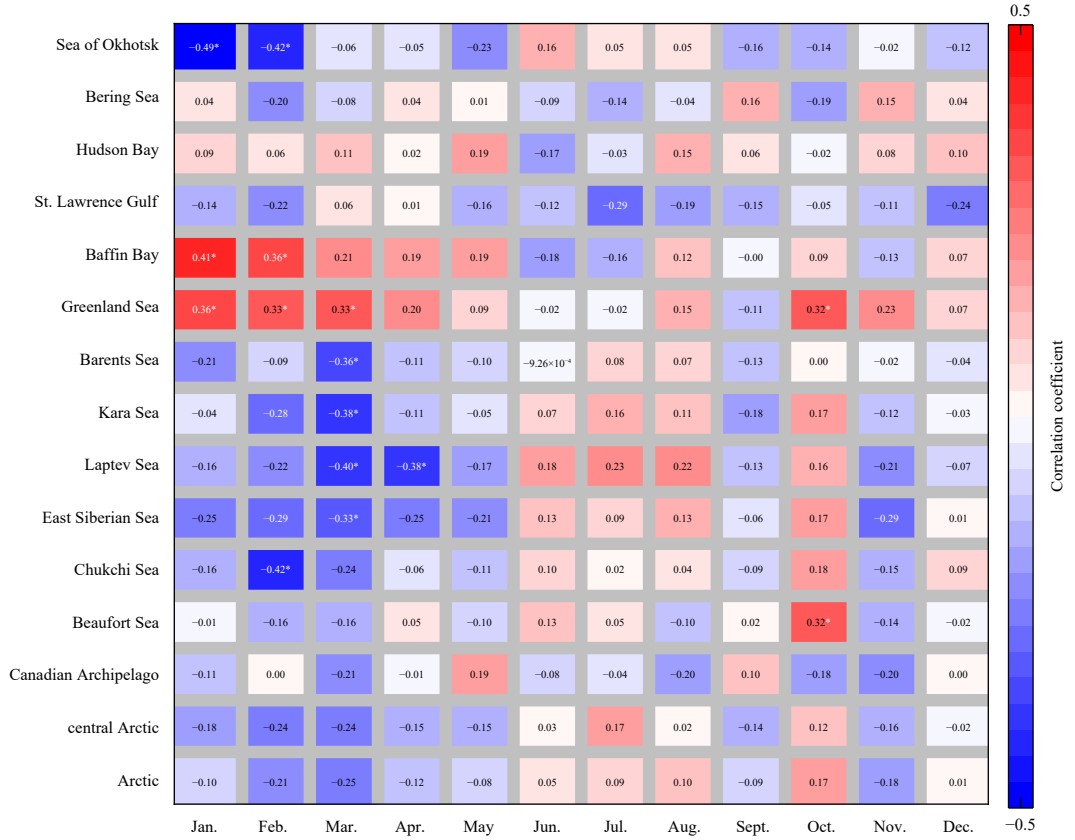

Fig. 7. Pearson correlations between the melt onset dates of different Arctic sub-regions and monthly Arctic Oscillation (AO). * indicates statistically significant correlation at a 95% confidence level.

Table 1. Correlation coefficients between the Arctic Oscillation (AO) index (winter: January–March, spring: April–June, and summer: July–September) with respect to melt onset dates (MOD) during 1979–2017 for the Arctic and its sub-regions

Region	Jan.–Mar. AO & MOD	Apr.–Jun. AO & MOD	Jul.–Sept. AO & MOD
Sea of Okhotsk	−0.43*	−0.08	−0.06
Bering Sea	−0.11	−0.01	0.01
Hudson Bay	0.11	0.03	0.12
St. Lawrence Gulf	−0.14	−0.14	−0.38*
Baffin Bay	0.44*	0.14	−0.01
Greenland Sea	0.45*	0.17	0.00
Barents Sea	−0.28	−0.13	−0.01
Kara Sea	−0.31	−0.06	0.03
Laptev Sea	−0.34*	−0.25	0.17
East Siberian Sea	−0.39*	−0.21	0.09
Chukchi Sea	−0.36*	−0.05	−0.03
Beaufort Sea	−0.15	0.04	−0.02
Canadian Archipelago	−0.13	0.06	−0.07
Central Arctic	−0.29	−0.17	0.01
Arctic	−0.24	−0.10	0.05

Note: * indicates statistically significant correlation at a 95% confidence level.

and statistical methods (i.e., Sen's slope estimator, M-K mutation test, and correlation analysis). The main conclusions are summarized as follows:

(1) The spatial patterns of mean annual MOD have noticeable regional differences over the Arctic, as well as interannual trend variations. The mean annual MOD over Arctic sea ice is related to the latitude, and earlier MOD is generally located in the peripheral and southern regions of sea ice. Moreover, the MOD is trending universally earlier for the majority of Arctic sea ice from 1979 to 2017, while the magnitude of trend varies from region to region. In addition, the regions in the middle and high latitudes (Barents Sea, Kara Sea, Laptev Sea, East Siberian Sea, Chukchi Sea, Beaufort Sea, Canadian Archipelago, and central Arctic) dominate the variation of MOD in the Arctic.

(2) The mutations in temporal trends of annual MOD exhibit a complex and dynamic behavior during the past 39 years. Although some significant mutations have occurred in different sub-regions, there is no direct connection between them. Therefore, it is inferred that the regional extreme variation of MOD is likely related to their local atmospheric conditions and activities. Besides, the mutation in sub-regions does not have a significant impact on the overall Arctic mutation.

(3) The response of MOD to AO varies greatly in different regions. The seasonal AO has more influence on MOD than monthly AO. The MOD has a negative correlation with winter AO in most Arctic sub-regions except for Baffin Bay and Greenland Sea. The MOD may be affected by many factors (e.g., air temperature, and ocean heat flux) leading to the weak correlation between MOD and AO, which is worthy of further investigation in the future.

Our results show that the effects of the mutations and variation on the temporal trends of MOD over Arctic sea ice are complex and dynamic during the past 39 years. In summary, while these preliminary results look promising, this study does not fully explore the physical mechanism that affects MOD variation from the aspect of large-scale atmospheric circulation. Further analysis of the MOD patterns in each region and their relationship to the atmospheric conditions is necessary to thoroughly explain the causes of the variability in MOD at a large scale. In the future, the effect of atmospheric circulation changes on the MOD and the length of the melt season will be further investigated (Ballinger et al., 2019; Huang et al., 2019; Stroeve et al., 2014), which will help us to get a better and more complete understanding of the physical processes controlling the evolution of sea ice melt and break-up patterns, and in turn improve the accuracy of global climate model predictions.

Acknowledgements

We thank NSIDC and NOAA for making the MOD and AO index data publicly available respectively. The MOD data used in the study are obtained from NSIDC (https://nsidc.org/data/nsidc-0105) and the AO index data are from NOAA National Centers for Environmental Information (http://ncdc.noaa.gov/teleconnections/ao/).

References

Aagaard K, Carmack E C. 1989. The role of sea ice and other fresh water in the Arctic circulation. Journal of Geophysical Research: Oceans, 94(C10): 14485–14498, doi: 10.1029/JC094iC10p14485

Abdalati W, Steffen K, Otto C, et al. 1995. Comparison of brightness temperatures from SSMI instruments on the DMSP F8 and FII satellites for Antarctica and the Greenland ice sheet. International Journal of Remote Sensing, 16(7): 1223–1229, doi: 10.1080/01431169508954473

Anderson M R. 1987. The onset of spring melt in first-year ice regions of the Arctic as determined from scanning multichannel microwave radiometer data for 1979 and 1980. Journal of Geophysical Research: Oceans, 92(C12): 13153–13163, doi: 10.1029/JC092iC12p13153

Anderson M, Bliss A C, Drobot S. 2019. Snow melt onset over Arctic sea ice from SMMR and SSM/I-SSMIS brightness temperatures, Version 4. Boulder, CO: NASA National Snow and Ice Data Center Distributed Active Archive Center

Anderson M R, Drobot S D. 2001. Spatial and temporal variability in snowmelt onset over Arctic sea ice. Annals of Glaciology, 33: 74–78, doi: 10.3189/172756401781818284

Ballinger T J, Lee C C, Sheridan S C, et al. 2019. Subseasonal atmospheric regimes and ocean background forcing of Pacific Arctic sea ice melt onset. Climate Dynamics, 52(9–10): 5657–5672, doi: 10.1007/s00382-018-4467-x

Barber D G, Thomas A. 1998. The influence of cloud cover on the radiation budget, physical properties, and microwave scattering coefficient (/spl sigma//spl deg/) of first-year and multiyear sea ice. IEEE Transactions on Geoscience and Remote Sensing, 36(1): 38–50, doi: 10.1109/36.655316

Barry R G, Serreze M C, Maslanik J A, et al. 1993. The Arctic sea ice-climate system: observations and modeling. Reviews of Geophysics, 31(4): 397–422, doi: 10.1029/93RG01998

Belchansky G I, Douglas D C, Mordvintsev I N, et al. 2004a. Estimating the time of melt onset and freeze onset over Arctic sea-ice area using active and passive microwave data. Remote Sensing of Environment, 92(1): 21–39, doi: 10.1016/j.rse.2004.05.001

Belchansky G I, Douglas D C, Platonov N G. 2004b. Duration of the Arctic sea ice melt season: regional and interannual variability, 1979–2001. Journal of Climate, 17(1): 67–80, doi: 10.1175/1520-0442(2004)017<0067:DOTASI>2.0.CO;2

Bi Haibo, Fu Min, Sun Ke, et al. 2016. Arctic sea ice thickness changes in terms of sea ice age. Acta Oceanologica Sinica, 35(10): 1–10, doi: 10.1007/s13131-016-0922-x

Bi Haibo, Yang Qinghua, Liang Xi, et al. 2019. Contributions of advection and melting processes to the decline in sea ice in the Pacific sector of the Arctic Ocean. The Cryosphere, 13(5): 1423–1439, doi: 10.5194/tc-13-1423-2019

Bliss A C, Anderson M R. 2014a. Daily area of snow melt onset on Arctic sea ice from passive microwave satellite observations 1979–2012. Remote Sensing, 6(11): 11283–11314, doi: 10.3390/rs61111283

Bliss A C, Anderson M R. 2014b. Snowmelt onset over Arctic sea ice from passive microwave satellite data: 1979–2012. The Cryosphere, 8(6): 2089–2100, doi: 10.5194/tc-8-2089-2014

Bliss A C, Anderson M R. 2018. Arctic sea ice melt onset timing from passive microwave-based and surface air temperature-based methods. Journal of Geophysical Research: Atmospheres, 123(17): 9063–9080, doi: 10.1029/2018JD028676

Bliss A C, Miller J A, Meier W N. 2017. Comparison of passive microwave-derived early melt onset records on Arctic sea ice. Remote Sensing, 9(3): 199, doi: 10.3390/rs9030199

Bliss A C, Steele M, Peng Ge, et al. 2019. Regional variability of Arctic sea ice seasonal change climate indicators from a passive microwave climate data record. Environmental Research Letters, 14(4): 045003, doi: 10.1088/1748-9326/aafb84

Box J E, Colgan W T, Christensen T R, et al. 2019. Key indicators of Arctic climate change: 1971–2017. Environmental Research Letters, 14(4): 045010, doi: 10.1088/1748-9326/aafclb

Chen Shangfeng, Yu Bin, Chen Wen. 2014. An analysis on the physical process of the influence of AO on ENSO. Climate Dynamics, 42(3–4): 973–989, doi: 10.1007/s00382-012-1654-z

Cohen J, Screen J A, Furtado J C, et al. 2014. Recent Arctic amplification and extreme mid-latitude weather. Nature Geoscience, 7(9): 627–637, doi: 10.1038/NGEO2234

Curry J A, Schramm J L, Ebert E E. 1995. Sea ice-albedo climate feedback mechanism. Journal of Climate, 8(2): 240–247, doi: 10.1175/1520-0442(1995)008<0240:SIACFM>2.0.CO;2

Da Silva R M, Santos C A G, Moreira M, et al. 2015. Rainfall and river flow trends using Mann–Kendall and Sen's slope estimator statistical tests in the Cobres River basin. Natural Hazards, 77(2): 1205–1221, doi: 10.1007/s11069-015-1644-7

Drobot S D, Anderson M R. 2001a. An improved method for determining snowmelt onset dates over Arctic sea ice using scanning multichannel microwave radiometer and special sensor microwave/imager data. Journal of Geophysical Research: Atmospheres, 106(D20): 24033–24049, doi: 10.1029/2000JD000171

Drobot S D, Anderson M R. 2001b. Comparison of interannual snowmelt-onset dates with atmospheric conditions. Annals of Glaciology, 33: 79–84, doi: 10.3189/172756401781818851

Fu Guobin, Yu Jingjie, Yu Xiubo, et al. 2013. Temporal variation of extreme rainfall events in China, 1961–2009. Journal of Hydrology, 487: 48–59, doi: 10.1016/j.jhydrol.2013.02.021

Huang Yiyi, Dong Xiquan, Xi Baike, et al. 2019. A survey of the atmospheric physical processes key to the onset of Arctic sea ice melt in spring. Climate Dynamics, 52(7–8): 4907–4922, doi: 10.1007/s00382-018-4422-x

Jevrejeva S, Moore J C, Grinsted A. 2003. Influence of the Arctic Oscillation and El Niño-Southern Oscillation (ENSO) on ice conditions in the Baltic Sea: the wavelet approach. Journal of Geophysical Research: Atmospheres, 108(D21): 4677, doi: 10.1029/2003JD003417

Jezek K C, Merry C, Cavalieri D, et al. 1991. Comparison between SMMR and SSM/I Passive Microwave Data Collected over the Antarctic Ice Sheet. Columbus, NY: Byrd Polar Research Center, The Ohio State University, 1–62

Kendall M G. 1948. Rank Correlation Methods. London: Charles Griffin

Kwok R, Cunningham G F, Nghiem S V. 2003. A study of the onset of melt over the Arctic Ocean in RADARSAT synthetic aperture radar data. Journal of Geophysical Research: Oceans, 108(C11): 3363, doi: 10.1029/2002JC001363

Lemke P, Ren J, Alley R B, et al. 2007. Observations: changes in snow, ice and frozen ground, climate change 2007: the physical science basis. In: Solomon S, Qin D, Manning M, et al, eds. Contribution of Working Group I to the Fourth Assessment Report of the Intergovernmental Panel on Climate Change. Cambridge: Cambridge University Press, 337–383

Liuzzo L, Bono E, Sammartano V, et al. 2016. Analysis of spatial and temporal rainfall trends in Sicily during the 1921–2012 period. Theoretical and Applied Climatology, 126(1–2): 113–129, doi: 10.1007/s00704-015-1561-4

Maksimovich E, Vihma T. 2012. The effect of surface heat fluxes on interannual variability in the spring onset of snow melt in the central Arctic Ocean. Journal of Geophysical Research: Oceans, 117(C7): C07012, doi: 10.1029/2011JC007220

Mann H B. 1945. Nonparametric tests against trend. Econometrica, 13(3): 245–259, doi: 10.2307/1907187

Markus T, Stroeve J C, Miller J. 2009. Recent changes in Arctic sea ice melt onset, freezeup, and melt season length. Journal of Geophysical Research: Oceans, 114(C12): C12024, doi: 10.1029/2009JC005436

Meier W, Fetterer F, Duerr R, et al. 2017. NOAA/NSIDC climate data record of passive microwave sea ice concentration, Version 3. Boulder, CO: National Snow and Ice Data Center

Moritz R E, Bitz C M, Steig E J. 2002. Dynamics of recent climate change in the Arctic. Science, 297(5586): 1497–1502, doi: 10.1126/science.1076522

Mortin J, Svensson G, Graversen R G, et al. 2016. Melt onset over Arctic sea ice controlled by atmospheric moisture transport. Geophysical Research Letters, 43: 6636–6642, doi: 10.1002/2016GL069330

Pachauri R K, Allen M R, Barros V R, et al. 2014. Climate change 2014: synthesis report. In: Contribution of Working Groups I, II and III to the fifth assessment report of the Intergovernmental Panel on Climate Change. Geneva: IPCC

Perovich D K, Nghiem S V, Markus T, et al. 2007. Seasonal evolution and interannual variability of the local solar energy absorbed by the Arctic sea ice–ocean system. Journal of Geophysical Research: Oceans, 112, doi: 10.1029/2006JC003558

Rigor I G, Colony R L, Martin S. 2000. Variations in surface air temperature observations in the Arctic, 1979–97. Journal of Climate, 13(5): 896–914, doi: 10.1175/1520-0442(2000)013<0896:visato>2.0.co;2

Rigor I G, Wallace J M, Colony R L. 2002. Response of sea ice to the Arctic Oscillation. Journal of Climate, 15(18): 2648–2663, doi: 10.1175/1520-0442(2002)015<2648:ROSITT>2.0.CO;2

Sen P K. 1968. Estimates of the regression coefficient based on Kendall's tau. Journal of the American statistical association, 63: 1379–1389, doi: 10.2307/2285891

Singh R K, Singh T V, Singh U S. 2020. Long-term observation of the Arctic sea ice melt onset from microwave radiometry. Journal of the Indian Society of Remote Sensing, 1–8, doi: 10.1007/s12524-020-01220-6

Smith D M. 1998. Observation of perennial Arctic sea ice melt and freeze-up using passive microwave data. Journal of Geophysical Research: Oceans, 103: 27753–27769, doi: 10.1029/98jc02416

Stroeve J C, Markus T, Boisvert L, et al. 2014. Changes in Arctic melt season and implications for sea ice loss. Geophysical Research Letters, 41: 1216–1225, doi: 10.1002/2013GL058951

Stroeve J, Markus T, Meier W N, et al. 2006. Recent changes in the Arctic melt season. Annals of Glaciology, 44: 367–374, doi: 10.1002/2013gl058951

Stroeve J, Maslanik J, Li X. 1998. An intercomparison of DMSP F11- and F13-derived sea ice products. Remote Sensing of Environment, 64: 132–152, doi: 10.1016/s0034-4257(97)00174-0

Stroeve J, Notz D. 2018. Changing state of Arctic sea ice across all seasons. Environmental Research Letters, 13: 103001, doi: 10.1088/1748-9326/aade56

Thompson D W J, Wallace J M. 1998. The Arctic Oscillation signature in the wintertime geopotential height and temperature fields. Geophysical research letters, 25(9): 1297–1300, doi: 10.1029/98gl00950

Wang Y, Bi H, Huang H, et al. 2019. Satellite-observed trends in the Arctic sea ice concentration for the period 1979–2016. Journal of Oceanology and Limnology, 37(1): 18–37, doi: 10.1007/s00343-019-7284-0

Winebrenner D P, Nelson E D, Colony R, et al. 1994. Observation of melt onset on multiyear Arctic sea ice using the ERS 1 synthetic aperture radar. Journal of Geophysical Research: Oceans, 99: 22425–22441, doi: 10.1029/94jc01268